White Rose Research Online
eprints@whiterose.ac.uk
https://eprints.whiterose.ac.uk
Universities of Leeds, Sheffield and York

Deposited via The University of Sheffield.

White Rose Research Online URL for this paper:
https://eprints.whiterose.ac.uk/id/eprint/909/

Article:

Plimmer, S.A., David, J.P.R., Grey, R. et al. (2000) Avalanche multiplication in AlxGa1-xAs (x=0to0.60). IEEE Transactions on Electron Devices, 47 (5). pp. 1089-1097. ISSN: 0018-9383

https://doi.org/10.1109/16.841245

Reuse

Items deposited in White Rose Research Online are protected by copyright, with all rights reserved unless indicated otherwise. They may be downloaded and/or printed for private study, or other acts as permitted by national copyright laws. The publisher or other rights holders may allow further reproduction and re-use of the full text version. This is indicated by the licence information on the White Rose Research Online record for the item.

Takedown

If you consider content in White Rose Research Online to be in breach of UK law, please notify us by emailing eprints@whiterose.ac.uk including the URL of the record and the reason for the withdrawal request.

UNIVERSITY OF LEEDS
University of Sheffield
UNIVERSITY of York

Avalanche Multiplication in $Al_xGa_{1-x}As$ $(x = 0 to 0.60)$

Stephen A. Plimmer, J. P. R. David, R. Grey, and G. J. Rees

Abstract—**Electron and hole multiplication characteristics, M_e and M_h, have been measured in $Al_xGa_{1-x}As$ ($x = 0$–0.60) homojunction p^+-i-n^+ diodes with i-region thicknesses, w, from 1 μm to 0.025 μm and analyzed using a Monte Carlo model (MC). The effect of the composition on both the macroscopic multiplication characteristics and microscopic behavior is therefore shown for the first time. Increasing the alloy fraction causes the multiplication curves to be shifted to higher voltages such that the multiplication curves at any given thickness are practically parallel for different x. The M_e/M_h ratio also decreases as x increases, varying from ~2 to ~1 as x increases from 0 to 0.60 in a $w = 1$ μm p^+-i-n^+. The Monte-Carlo model is also used to extract ionization coefficients and dead-space distances from the measured results which cover electric field ranges from ~250 kV/cm–1200 kV/cm in each composition. These parameters can be used to calculate the nonlocal multiplication process by solving recurrence equations. Limitations to the applicability of field-dependent ionization coefficients are shown to arise however when the electric-field profile becomes highly nonuniform.**

Index Terms—**Avalanche diodes, avalanche photodiodes, hot carriers, impact ionization, Monte Carlo methods.**

I. Introduction

Avalanche multiplication in $Al_xGa_{1-x}As$ is important in semiconductor devices operating at high electric fields such as heterojunction bipolar transistors (HBT's) [1] and IMPATT's [2] since it limits the power performance. Accurate knowledge of the avalanche multiplication process in this material system is therefore required for a variety of device design purposes.

Several experimental breakdown studies have been carried out in $Al_xGa_{1-x}As$ including the first measurements of the breakdown voltages in one-sided junctions over the alloy composition range $x = 0$ to 0.27 by Yeh and Liu [3]. David *et al.* [4] measured the electron and hole initiated multiplication, M_e and M_h respectively, in P^+-N-N^+ heterostructures with $Al_xGa_{1-x}As$ ($x = 0$ to 0.60) high field regions and GaAs cladding regions. They deduced the electron and hole ionization coefficients, which are the mean of the inverse distance between electron and hole ionization collisions, α and β, respectively. Both these works show that as the composition increases the magnitude of α and β decrease while [4] shows the α/β ratio decreases such that $\beta > \alpha$ for $x > 0.3$. Robbins *et al.* [5] measured α and β from abrupt one-sided homojunctions with $x = 0$ to 0.40 and found reasonable agreement with [4] except that $\alpha > \beta$ for all alloys. In [4], [5] however, local ionization theory was used to deduce α and β whereby these parameters are assumed to vary with solely the local electric field. While this analysis can be justified in devices with thick avalanche regions, such that most carriers are in equilibrium with the field, the avalanche regions of modern transistors can be < 1 μm [6]. In thin structures or where the electric field is highly nonuniform, nonlocal effects become important in determining the multiplication. Moreover, there is very little published multiplication data to date from electric fields > 500 kV/cm.

We have already shown that the local ionization model (LM) overestimates the measured multiplication in $Al_xGa_{1-x}As$ $(x = 0-0.30)$ p^+-i-n^+s when $w < 0.5$ μm [7], [8], especially at low applied voltages. Furthermore, it is incapable of predicting the excess noise figures of thin GaAs and $Al_xGa_{1-x}As$ APD's as shown, for example, in [9], [10]. The overestimation of both the multiplication and the excess noise in thin structures by the LM has been explained by its neglect of the dead-space distance, d, where carriers have insufficient energy to initiate ionization. Quantifying the avalanche multiplication process in the presence of significant dead-space effects, however, is not straightforward. Since dead-space has a different effect in each geometry, it causes the local ionization coefficients to differ when they are deduced from photomultiplication measurements on thin devices with different electric field profiles. One attempt to circumvent this problem involves presenting a different parameterized form for the ionization coefficient deduced from each measured device in the manner of Lennox *et al.* [11]. However, the accuracy of interpolating or extrapolating these data to model general device geometries is still unclear. Another approach has been to modify the LM to include dead-space by changing the limits over which ionization is assumed to occur in the multiplication region (see for example [6], [12]). However, this treatment still does not fully account for its effect as shown in [13] while it is also unsuitable for calculating the excess noise figure of a thin structures, where the results are determined by the spatial distribution of ionization events [10]. Consequently, the ionization coefficients published to date are inapplicable to submicron devices.

A rigorous account of dead-space effects can be made by using the recursive technique developed by the Wisconsin group which allows both the multiplication and excess noise to be given from "microscopic" ionization coefficients, α^* and β^*

Manuscript received October 8, 1999; revised October 8, 1999. The theoretical work was supported by EPSRC (UK) Grant GR/L71674 and the experimental work was supported by DERA, Malvern, U.K. The review of this paper was arranged by Editor J. N. Hollenhorst.

The authors are with the Department of Electronic and Electrical Engineering, University of Sheffield, Sheffield, U.K. S1 3JD (e-mail: s.a.plimmer@sheffield.ac.uk).

Publisher Item Identifier S 0018-9383(00)02733-7.

0018-9383/00$10.00 © 2000 IEEE

[14], [15]. These coefficients are defined as the ionization probability per unit distance experienced by an electron or hole, respectively, after travelling for the dead-space distance. Unlike the local parameters which depend on the device geometry when dead-space becomes significant, the "microscopic" ones are always device independent, which allows the avalanche process to be quantified unambiguously. The recursive technique accounts for the fact that all carriers must travel for a dead-space distance before they are able to initiate ionization. Consequently, α^* and β^* are generally different to α and β but the relationship between them is not straightforward. Since experimentalists have not used this recursive technique to analyze their results to date, no reliable data exists which can be used for calculations of the avalanche multiplication process in sub-micron devices. Moreover, it is apparent that these differences between the "local" and "microscopic" ionization coefficients and their applicability to different models has led to some confusion in the literature as described in [13], [16].

In this work we deduce the device-independent "microscopic" ionization coefficients and dead-space distances from previously measured multiplication results on $Al_xGa_{1-x}As$ $(0 < x < 0.3)$ p^+-i-n^+ diodes as well as a new series of .$Al_{0.60}Ga_{0.40}As$ p^+-i-n^+s with i-region thicknesses, w, from 1 μm down to 0.025 μm. This is done with the aid of an MC model where the history of carriers is explicitly accounted for, instead of either a local model or one of recursive techniques discussed above, where position dependent ionization probabilities are assumed to depend on the local electric field. This combination of extensive measurements on 31 layers and the MC analysis allows the effect of composition on both the bulk *and* the nonlocal multiplication behavior to be quantified accurately for the first time. The effect of composition on the microscopic multiplication process is also illustrated. The data can be used with the recursive technique described previously to give the multiplication properties in devices which access electric fields about double those conventionally covered by published photomultiplication measurements. We also illustrate general limitations to the applicability of these data.

II. Experimental Details

The growth, fabrication and characterization procedures for $Al_{0.60}Ga_{0.40}As$ were very similar to those described $Al_xGa_{1-x}As$ $(x = 0 - 0.30)$ as explained in [7], [8] and so only a general resume is given here. To study electron multiplication, homojunction p^+-i-n^+s were grown with alloy compositions $x = 0$, 0.15, 0.3 and 0.6 and i-region thicknesses of $w = 1$ μm, 0.5 μm, 0.1 μm, 0.05 μm, and 0.025 μm using conventional solid-source molecular beam epitaxy. To study hole multiplication, via-holes were etched into the substrate of some devices to allow optical access to the n-regions for the injection of primary hole currents. However, this sometimes caused the devices to degrade as evidenced by increased dark currents. Moreover, the hole quantum efficiency in the $Al_{0.60}Ga_{0.40}As$ samples was found to be very low leading to low photocurrents. Therefore, hole multiplication was also investigated by growing several n^+-i-p^+s. Because avalanche multiplication characteristics depend critically on the electric field profile, the i-region thickness, w, the P^+ and N^+ cladding doping levels, p and n, and the unintended i-region doping, i, were deduced by adjusting these parameters in a solution of Poisson's equation to fit the measured capacitance–voltage (*C–V*) profiles from all layers. The accuracy of the results was verified by secondary ion mass spectrometry (SIMS) measurements on some of the devices from which we estimate that w can be obtained to within 1–2% certainty and p and n to within 10–50%.

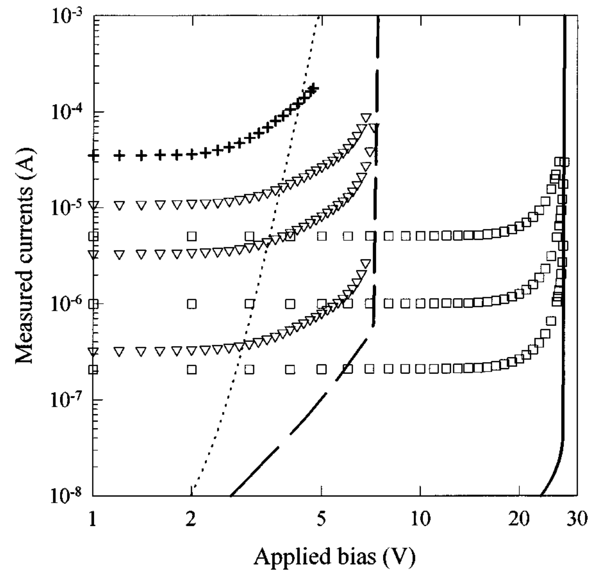

Fig. 1. Three measured photocurrents (open symbols) and a measured dark current (lines) from the $Al_{.60}Ga_{0.40}As$ samples with $w = 0.5$ μm (□, ——) and $w = 0.05$ μm (∇, — —). Also shown are a typical photocurrent (+) and dark current (- - -) measured from a $w = 0.05$ μm GaAs device.

To measure the photomultiplication characteristics themselves, the wavelength of light was chosen to ensure that practically all photons are absorbed in the cladding regions and the primary photocurrents are therefore purely electron-type or hole-type. (633 nm light was used in GaAs, 542 nm light was used in $Al_{0.15}Ga_{0.85}As$ and 442 nm light in $Al_xGa_{1-x}As$ (x = 0.3 and 0.6)). To ensure only the multiplied primary photocurrents were measured, the incident light was chopped and the resulting a.c. photocurrent was detected using a lock in amplifier. Measurements were undertaken on each layer at primary photocurrent levels of between 50 nA and 50 μA to confirm the absence of effects due to space-charge or diode resistance. To obtain M_e and M_h, the measured photocurrent-voltage curves had to be corrected for a small ($\approx$ 1%) increase in the photocurrent as the bias increased from zero to that corresponding to the onset of multiplication. This effect is due to the increase in collection efficiency which arises when the depletion region extends into the contacts with increasing bias as described by Woods *et al.* [17]. Reproducible M_e and/or M_h curves were obtained from all diodes.

A range of the measured photocurrent characteristics from the $w = 0.5$ μm and 0.05 μm $Al_{0.60}Ga_{0.40}As$ p^+-i-n^+s are shown in Fig. 1 along with a typical dark current, I_d, from 200 μm radius devices showing that this is several orders of magnitude lower than the photocurrent. Also shown on this plot for comparison are a typical photocurrent and dark current measured from

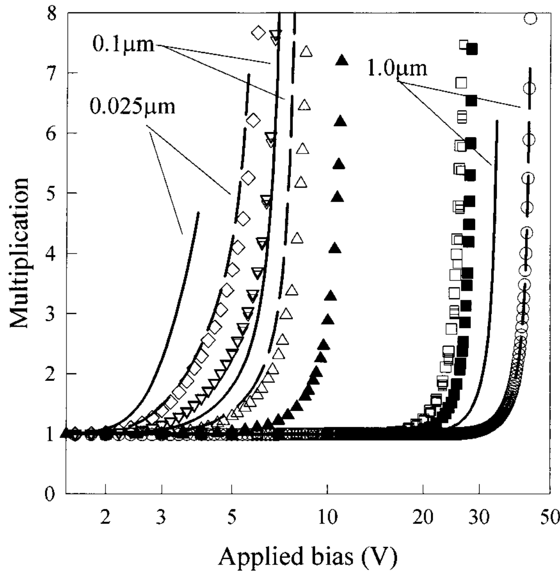

Fig. 2. M_e from $Al_{60}Ga_{40}As$ p^+-i-n^+s with $w = 1$ μm (o), 0.5 μm (□), 0.1 μm (△), 0.05 μm (▽), 0.025 (◇) and M_h from n^+-i-p^+s with $w = 0.5$ μm (■) and 0.1 μm (▲). Also shown are measured M_e from GaAs (——) and $Al_{0.30}Ga_{0.70}As$ (- - -) p^+-i-n^+s with $w = 1$ μm, 0.1 μm and 0.025 μm as labeled on the graph.

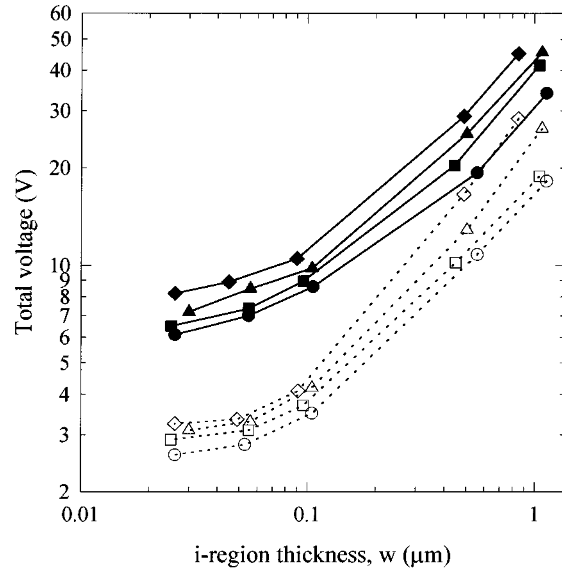

Fig. 3. The total voltage (including the built in voltage) at breakdown (filled symbols) and the onset of measurable multiplication (open symbols) versus i-region thickness for the investigated compositions. The different symbols represent the different alloy fractions: $x = 0$ (o, •), $x = 0.15$ (□, ■), $x = 0.30$ (△, ▲) and $x = 0.60$ (◇, ♦). Lines are to guide the eye.

the $w = 0.05$ μm GaAs p^+-i-n^+. These data illustrate the rapid increase in I_d which was seen in the ultrathin GaAs structures due to tunnelling and the much lower dark currents in devices of the same thickness but with a wider band-gap. After normalization, the three photocurrent curves from the $Al_{0.60}Ga_{0.40}As$ $w = 0.5$ μm device and the three from the 0.05 μm device in Fig. 1 are indistinguishable as shown in Fig. 2. The M_e (M_h) from the other investigated p^+-i-n^+s (n^+-i-p^+s) of this alloy composition are also shown in Fig. 2 along with the measured M_e characteristics of the GaAs and $Al_{0.30}Ga_{0.70}As$ p^+-i-n^+s which have $w = 1$ μm, 0.1 μm and 0.025 μm for comparison. In the GaAs devices with $w < 0.1$ μm, the tunnelling currents limited the highest measurable M_e to ≈ 5. By contrast, in the ultrathin $Al_xGa_{1-x}As$ ($x \geq 0.3$) diodes where tunnelling effects are insignificant, multiplication values of typically 15–30 could be achieved. The effect of composition on the multiplication cannot be concluded from Fig. 2, since there is no clear trend in the results. This is because there are small but significant variations in the field profiles of devices with different x but the same nominal w. It indicates that the electric field profile should be accounted for as accurately as possible and thus motivates the use of the Monte Carlo model.

A clearer trend can be seen in Fig. 3 where the total breakdown voltage, V_{bd}, including the built-in voltage (which is assumed to vary linearly with x from 1.2 V in GaAs up to 1.65 V in $Al_{0.60}Ga_{0.40}As$) is plotted against w, as determined by modeling the measured *C–V* profiles for all diodes. The relative change in V_{bd} with x is practically the same for any given thickness. Furthermore, the total voltage corresponding to the onset of measured multiplication, defined arbitrarily as $M_e = 1.0024$ for consistency, scales with the composition in a similar way such that the relative effect of changing the alloy fraction appears similar for all thicknesses (also shown on Fig. 3). Compared to a GaAs device of the same thickness, the V_{bd} of an $Al_{0.30}Ga_{0.70}As$ p^+-i-n^+ is approximately 15% higher while it is 30% higher in an $Al_{0.60}Ga_{0.40}As$ p^+-i-n^+.

This graph implies that the multiplication curves from a set of equal thickness devices of various compositions will be approximately parallel. However, to extract further information about the ionization process, it is necessary to model the measured results while accurately accounting for the effect of the electric field profiles. It has been shown by Scrobhaci and Tang [18] that the ionization probability at any point in a structure depends not on the only the field at that point but also the effect of the field on the carrier distribution function at previous points in the carrier's history. This means that it is inappropriate to use most of analysis procedures used to date which assume that ionization coefficients or probabilities depend only on solely the electric field: it is necessary instead to use a Monte Carlo model where the carrier history is implicitly included.

III. Monte Carlo Modeling

Modeling of the measured results would ideally be carried out using an MC model that incorporates realistic band-structures, but these are highly computer intensive and consequently impractical for our purposes of fitting to measured data. Therefore, we use an MC model described previously in [16] where the transport is described using effective dispersion relations which take the form $E(1 + \alpha_\varepsilon E) = h^2k^2/2m^*$ where E is kinetic energy, α_ε is a nonparabolicity factor, k is wavevector and m^* is the mass at the valley minima for both electrons and holes. (This model is different to the one we reported in [30] which used parabolic effective dispersion curves and, consequently, slightly overestimated the increase in multiplication with bias.) The masses and nonparabolicity factors are adjustable parameters that were chosen to reflect a "realistic" average mass versus average kinetic energy relationship. In all compositions, $m^* = 0.4m_o$ where m_o is the free electron mass while values of a_ε

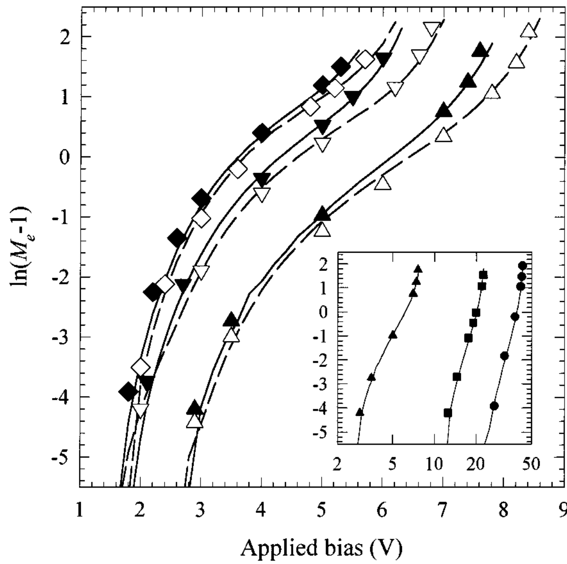

Fig. 4. MC fit (symbols) to measured M_e (lines) in the submicron $Al_{0.30}Ga_{0.70}As$ (closed symbols, ——) and $Al_{0.60}Ga_{0.40}As$ p^+-i-n^+s (open symbols, - - -) with $w = 0.1$ μm (Δ, ▲), 0.05 μm (∇, ▼), and 0.025 μm ($\Diamond$, ◆). Inset are the fits to Me for the $Al_{0.30}Ga_{0.70}As$ p^+-i-n^+s with $w = 1$ μm (•), 0.5 μm (■), and 0.1 μm (▲) to illustrate the fit quality across the range of diodes.

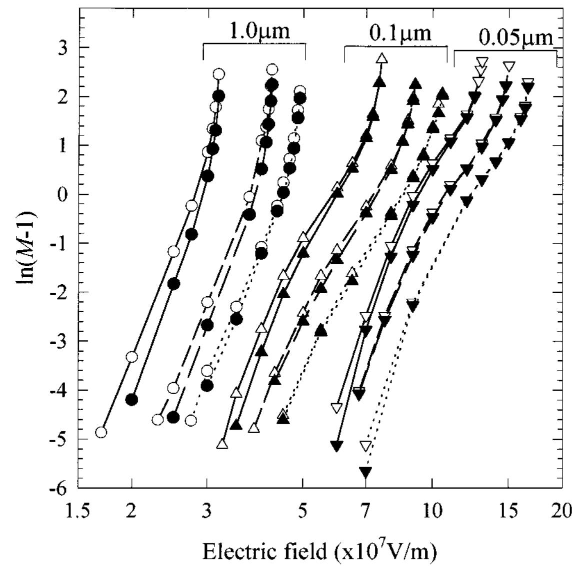

Fig. 5. MC-simulated M_e (open symbols) and M_h (closed symbols) curves plotted as $\ln(M-1)$ for ideal p^+-i-n^+s of GaAs (——), $Al_{0.30}Ga_{0.70}As$ (— —), and $Al_{0.60}Ga_{0.40}As$ (- - -) with $w = 1$ μm (∘, •), 0.1 μm (Δ, ▲), and 0.05 μm (∇, ▼).

varied between 0.35 and 0.43. A parameter that describes the coupling strength of the phonon scattering rate was also adjusted to allow exact fits to the measured multiplication data. The ionization rate is included as a scattering mechanism for energies E greater than the minimum threshold energy for ionization, E_{th}, and takes the form used by Stobbe *et al.* [19]

$$R_{ii} = C_{ii}\left[\frac{E - E_{th}}{E_{th}}\right]^4 \tag{1}$$

where E_{th} is taken to be the average band-gap of the first conduction band of the material defined after Allam [20] as $E_{th} = 1/8E_\Gamma + 4/8E_L + 3/8E_X$ where E_Γ, E_L and E_X are the energy gaps from the valence band minima to the $1\Gamma, 4L$ and $3X$ conduction band minima, respectively. The ionization softness factor C_{ii} is another fitting parameter to experiment which is in the range from 3.6×10^{13}/s to 4.2×10^{13}/s in reasonable agreement with *ab initio* ionization rate calculations [19]. In [16], we report this model's ability to accurately simulate the avalanche process by it closely fitting the measured multiplication curves in GaAs p^+-i-n^+s with w as thin as 0.025 μm and p^+-n junctions doped to 2.2×10^{17} cm^{-3}. The model can similarly reproduce the measured M_e and M_h curves in submicron $Al_xGa_{1-x}As$ ($x = 0.15$ to 0.60) devices as shown in Fig. 4 where data are plotted for the $x = 0.30$ and 0.60 diodes as $\ln(M_e - 1)$ to emphasise the agreement for multiplication values as low as ≈ 1.01.

Since this is a simplified transport model, it is important to ensure that the model is not fitting the multiplication by producing errors in the dead-space which are compensated for by errors in the subsequent ionization probability. For a given $Al_xGa_{1-x}As$ composition, if we compare different width devices at the same electric field, the dead space to avalanche region width ratio would vary. However, the excellent agreement between the MC model and experiment strongly suggests that the model must be correctly predicting the dead space and the ionization probability. In [16] we also showed that this model reproduces the multiplication results in heavily doped GaAs p^+-n junctions which means that it must also correctly account for the carrier's history when the field is highly nonuniform. Whereas different combinations of adjustable parameters in the MC model can give the same mean ionization coefficients (i.e., the mean distance between ionization events) and replicate the multiplication characteristics in thick bulk structures, this is not true in submicron structures. The low multiplication characteristics of diodes with $w < 0.5$ μm are particularly sensitive to the choice of parameters, since these control both the magnitude of the dead-space and the way in which the ionization probability increases with increasing distance before reaching an equilibrium value. This result indicates that the only way that our model can replicate the measured multiplication is by giving the correct ionization PDF's, which include the dead-space values.

Once the model parameters have been determined by fitting to experiment, M_e and M_h were calculated for ranges of ideal p^+-i-n^+s to more clearly compare the effect of the alloy composition. These data for $x = 0$, 0.30 and 0.60 p^+-i-n^+s with $w = 1$ μm, 0.1 μm, and 0.05 μm are given in Fig. 5 to show that the effect of increasing the alloy fraction clearly shifts the multiplication curves to a higher applied electric field at each thickness. The same trend can be seen for M_e and M_h but at any given w the M_e/M_h ratio is closer to unity for a higher composition. The shift in the multiplication curves which occurs as x changes from 0 to 0.3 is very similar to the one when x changes from 0.3 to 0.6, indicating that the electron multiplication is not significantly affected by the semiconductor becoming indirect when $x > 0.42$ [21]. In fact, the breakdown voltage of the simulated ideal p^+-i-n^+s was found to be practically proportional to the average conduction band energy, E_{th}, for all thicknesses suggesting that the whole Brillouin zone affects these results rather than simply the minimum energy gap.

IV. Discussion

In this discussion, we believe that associating the effect of alloy fraction on the multiplication with changes in the individual material parameters in the Monte Carlo model would be inappropriate because these parameters are only applicable within the confines of this simplified model. Nevertheless, the fact the model clearly replicates the multiplication processes in the different materials allows the properties of these to be compared.

The simulated ideal p^+-i-n^+ results show that the effect of composition contrasts with the conventional one described in most solid state text books since Sze and Gibbons [22] whereby V_{bd} varies linearly with the energy gap of the minimum valley. Because Vbd continues to increase for compositions with $x > 0.42$, it is consistent instead with the description of the ionization process by Allam [20]; the carrier momenta of the initiating particles is argued to be completely randomized such that V_{bd} is determined by the average of the conduction band minima energies which represent the final electron states. The results of Figs. 3 and 4 also contrast with the results of Herbert *et al.* [23] where the V_{bd} in GaAs and Si was predicted to become less sensitive to material as the thickness decreases. By contrast, changing x by a given amount in $Al_xGa_{1-x}As$ causes V_{bd} to be changed by a similar fraction for any given thickness of p^+-i-n^+.

The results of Figs. 3 and 4 may be surprising considering that as the average band-gap and thus the ionization threshold and d become larger; one might expect V_{bd} in thick and thin structures to show a markedly different dependence on the alloy fraction. However, the phonon energy and the strength of phonon scattering also increase in such a way that d represents a smaller fraction of the mean distance between electron (hole) ionization collisions. Consequently, the effect of changing x is not readily apparent. The role of dead-space was therefore examined by calculating the spatial ionization coefficients for different thicknesses of ideal p^+-i-n^+ at a constant multiplication. These coefficients are evaluated from the fractional change in the spatial current flux, $J(x)$, by the expression (for electrons)

$$\alpha = \frac{1}{J_e(x)} \left\{ \left[\frac{dJ_e(x)}{dx} \right]_{\substack{electron\\ionization}} \right\} \quad (2)$$

with a similar expression for the hole coefficient, $\beta(x)$, in terms of J_h. It is noted that in (2) $dJ_e(x)/dx$ refers only to the change in $J_e(x)$ *due to electron ionization* between x and $x + dx$ and is not therefore the same as the $dJ_e(x)/dx$ term that appears in the current equations. We describe the behavior of these $\alpha(x)$'s and $\beta(x)$'s in terms of nonlocal effects in detail in [16] while their significance is that they are the coefficients which always return the multiplication when used in the current equations. In a purely local model without modifications for dead-space effects, both $\alpha(x)$ and $\beta(x)$ are assumed to be constant in an ideal p^+-i-n^+. For a constant value of multiplication, these parameters are plotted from the MC model in Fig. 6 for three $w = 1$ μm and three 0.1 μm ideal p^+-i-n^+s with $x = 0$, 0.3 and 0.6 with electrons injected at the left. The electric fields have been chosen such that $M_e = 5$ in all cases. The most striking overall feature

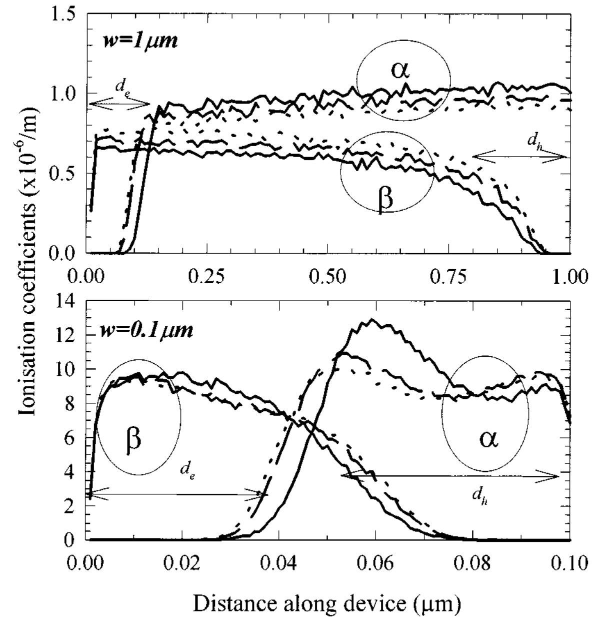

Fig. 6. Position dependent ionization coefficients in ideal $w = 1$ μm (top plot) and $w = 0.1$ μm (bottom plot) p^+-i-n^+s at $M_e = 5$ calculated using the MC model: GaAs (——), $Al_{0.30}Ga_{0.70}As$ (— —) and $Al_{0.60}Ga_{0.40}As$ (- - -). Dead-space regions are indicated on the plot.

of Fig. 6 is that the effect of composition appears small given the large range of ionization coefficient values covered by the two plots. For all three sets of data in the w = 1 μm plot, the electron dead-space, d_e, marked on the plot occupies about 10% of the device to the left of the plot for all compositions. For distances greater than this dead-space, $\alpha(x)$ increases quickly to assume an approximately constant value of 1×10^6 cm^{-3} for the rest of the structure. (The "local" description of a constant value is therefore a reasonable approximation for electrons in this thickness of p^+-i-n^+). However, holes that move from right to left give rise to plots of $\beta(x)$ which are somewhat different from the "local" behavior. Specifically, the hole dead-space distance, d_h, can be seen at the right of the plot but $\beta(x)$ exhibits a more gradual rise as holes travel at distances less than $w - d_h$. While the primary electrons in Fig. 6 are injected at the point $x = 0$, the secondary electrons and holes are created at various points throughout the device from $x = w$ to $x = 0$. The dead-space for the average secondary carrier therefore represents a bigger fraction of the distance between its creation point to the point where it is collected than for the primary electron, consequently it is more likely to exit the structure without ionizing. However, since electrons are injected, the secondary electrons represent a smaller fraction of the overall electron current than do the secondary holes as a fraction of the overall hole current. Consequently, the effect of dead-space on secondary electrons affects $\alpha(x)$ less than the effect of dead-space on secondary holes affects $\beta(x)$. To ensure that the slow rise in $\beta(x)$ is indeed due to the effect of dead-space being greater on the coefficient of the carrier type which was not injected a simulation was also carried out by injecting pure hole primaries at $x = w$. The resulting plots of $\alpha(x)$ and $\beta(x)$ mirror the results in Fig. 6 except that their shapes are reversed: the rise in $\beta(x)$ to its saturated level after the hole dead-space mirrors that of $\alpha(x)$ in Fig. 6 while the

rise in $\alpha(x)$ after the electron dead-space is gradual. This result indicates that the slow rise in the spatial coefficient is a feature of the opposite carrier-type to that injected, rather than specifically holes.

Nonlocal effects are more significant in the 0.1 μm structure as shown in the bottom plot of Fig. 6 where d_e $(\approx d_h)$ now represents about 50% of the overall device thickness. The device is now so thin that $\beta(x)$ is not able to attain an equilibrium value within its confines. Moreover, $\alpha(x)$ slightly "overshoots" its constant value for distances greater than d_e. This is interpreted as due to ionization by primary particles which initiate ionization without undergoing significant energy relaxation at very high electric fields [16]. The carriers consequently ionize coherently around the peak in $\alpha(x)$. Because the phonon scattering rates and phonon energies are greater in $Al_xGa_{1-x}As$ $(x \geq 0.3)$ than GaAs, the greater energy relaxation means the overshoot behavior is most pronounced in GaAs.

Despite subtle differences between alloy compositions in Fig. 6, the microscopic pictures shown here with the data in Figs. 3 and 5 suggest that the effect of increasing composition in $Al_xGa_{1-x}As$ $(x = 0 - 0.60)$ can be summarized as effectively shifting the multiplication process to a higher electric field for a diode of any given thickness. The multiplication characteristics are effectively displaced along the electric field axis for different x by a factor which is approximately proportional to E_{th}.

A similar comparison to the one we make here between different alloy fractions of $Al_xGa_{1-x}As$ was made between the measured curves from GaInP and GaAs p^+-i-n^+s by Ghin *et al.* [24]. That work showed that at a constant field the local ionization coefficients deduced from the GaInP devices were less affected by dead-space than those from the GaAs devices. In this respect, we also find the dead-space to be less significant as the composition and the average band-gap increase. For example, at 500 kV/cm the ratio of the dead-space to the mean distance between successive electron ionization events is 47% in GaAs, 20% in $Al_{0.30}Ga_{0.70}As$ and 13% in $Al_{0.60}Ga_{0.40}As$. As the average conduction band-gap and thus the ionization threshold energy of a semiconductor increases, it therefore appears that the absolute dead-space distance increases at any given field but the dead-space generally becomes a less significant fraction of the mean distance between ionization events for a given electric field. This leads to the local model being more successful in predicting the multiplication in materials with larger average band-gaps than those with narrow band-gaps for a given thickness of device. In [24] for example, Ghin *et al.* were able to use a local model to reproduce the measured multiplication in GaInP devices as thin as 0.1 μm whereas the local model underestimated the multiplication in a GaAs p^+-i-n^+ of the same thickness because of dead-space effects [7], [16].

V. Ionization Coefficients

The importance of differentiating between the ionization coefficients that enter the recursive equations and the local coefficients that are conventionally deduced from photomultiplication measurements is described by both Lacaita and Spinelli [13] and Plimmer *et al.* [16]. This distinction is necessary because dead-space effects cause the local ionization coefficients to be generally reduced below "microscopic" values by dead-space effects. In [16], we showed that "local" coefficients were heavily dependent on the thickness of the high field region as well as the field, F, for $F > 500$ kV/cm and so we termed these as "effective" rather than "local."

In this work, we address the ionization coefficient which should be used in the class of techniques that use microscopic ionization coefficients in a solution of recursive equations [14], [15] or an equivalent method which uses a random number generator described by Ong. *et al.* [25]. These techniques use the concept of the ionization probability distribution function, PDF, which is the probability that a carrier which is created or injected a distance $z = 0$ ionizes at a distance z downstream. PDF's are effectively histograms of the distances from creation that a carrier ionizes for the first time. For electrons, the PDF is given in terms of α^* by

$$\begin{aligned} \mathrm{PDF}_e(z) &= 0 \qquad z \leq d_e^* \\ \mathrm{PDF}_e(z) &= \alpha^* \exp\left[-\int_{d_e}^{z} \alpha^*\, dz\right] \cdot \qquad z > d_e^* \end{aligned} \tag{3}$$

while the same relations hold for the hole PDF with β^* and d_h^* replacing α^* and d_e^*, respectively. Equation (3) assumes that the ionization probability of any carrier is zero for its dead-space distance after injection and ionizes with the probability of $\alpha^*\, dz$ in each distance increment dz until it initiates ionization. α^* (β^*) is obtained in a straightforward way from a "Monte Carlo" ionization coefficient, which is the probability per unit distance of electron (hole) initiated ionization in a uniform electric field, α_{MC} (β_{MC}). The Monte Carlo coefficients are obtained by using the Monte Carlo model to simulate a single carrier in a infinite region of uniform electric field; their magnitude being the inverse mean distance an electron and hole travel between successive ionization events. α^* is given from α_{MC} by splitting the distance $1/\alpha_{MC}$ into a dead-space part from $z = 0$ to d_e^* where ionization is prohibited and then attributing the rest of the ionization events to distances beyond the dead-space, $z > d_e^*$, where carriers ionize with a spatial probability α^* leading to

$$\frac{1}{\alpha^*} = \frac{1}{\alpha_{MC}} = d_e^* \tag{4}$$

The same relation holds for holes in terms of β^*, β_{MC} and d_h^*. The Monte Carlo coefficients, which are also device-independent, are parameterized in Table I and plotted in Fig. 7 to show their decrease with increasing x. For all compositions, $\alpha_{MC} > \beta_{MC}$ although the α_{MC}/β_{MC} ratio decreases toward unity as x increases. The symbols on this plot denote calculated data points and the lines denote the parameterised expressions of Table I. Where PDFT's have been used to date, the electron (hole) dead-space distances are expressed in terms of an effective threshold energy, $E_{th\,(e)}^*$ $(E_{th\,(h)}^*)$, which is the minimum potential energy carriers must gain from the field to initiate ionization. We maintain this convention here so that in a uniform field, $F, d_e^* = E_{th\,(e)}^*/qF$ for electrons and $d_e^* = E_{th\,(h)}^*/qF$ for holes. To predict the effect of dead-space on the performance of GaAs APD, Hayat *et al.* [15] assumed E_{th}^* to equal the minimum threshold energies where the ionization rate increases

TABLE I
PARAMETERS FOR MICROSCOPIC ELECTRON (HOLE) IONIZATION COEFFICIENTS EXPRESSED AS $\alpha(\beta) = A \cdot \exp(-(B/F)^C)$, WHERE F IS THE ELECTRIC FIELD. DEAD-SPACE DISTANCES ARE ALSO GIVEN FOR ELECTRONS (HOLES) IN TERMS OF $E^*_{th\ (e)}$ ($E^*_{th\ (h)}$) AS DESCRIBED IN THE TEXT

Alloy, x	Type	E_{th}*	low $F < 6\text{x}10^7$V/m			high $F > 6\text{x}10^7$V/m		
			A	B	C	A	B	C
0.00	α	3.1	4.22x10^7	7.09x10^7	1.535	2.77x10^8	4.10x10^8	0.60
	β	3.3	5.89x10^7	8.89x10^7	1.402	2.27x10^8	3.12x10^8	0.687
0.15	α	3.2	3.36x10^8	2.35x10^8	1.0	1.26x10^8	1.80x10^8	1.0
	β	3.4	3.64x10^8	2.52x10^8	1.0	1.43x10^8	2.00x10^8	1.0
0.30	α	3.4	3.07x10^8	2.36x10^8	1.0	1.27x10^8	1.84x10^8	1.0
	β	3.6	3.43x10^8	2.53x10^8	1.0	1.36x10^8	1.99x10^8	1.0
0.60	α	3.4	3.47x10^8	2.82x10^8	1.0	1.39x10^8	2.27x10^8	1.0
	β	3.6	3.08x10^8	2.86x10^8	1.0	1.48x10^8	2.38x10^8	1.0

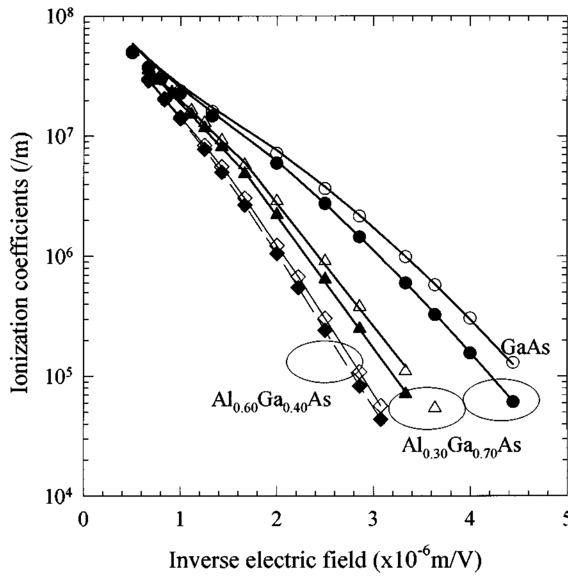

Fig. 7. αMC (open symbols) and β_{MC} (closed symbols) in GaAs (○, ●), $Al_{0.30}Ga_{0.70}As$ (△, ▲), and $Al_{0.60}Ga_{0.40}As$ (◇, ◆). Lines denote the parameterized expressions of Table I.

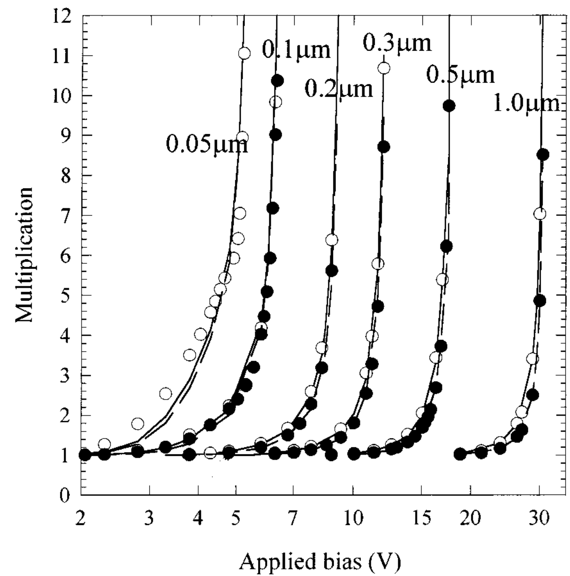

Fig. 8. Comparison of the GaAs MC-simulated M_e (——) and M_h (- -) and the PDFT-calculated M_e (open symbols) and M_h (filled symbols) for a range of ideal p$^+$-i-n$^+$s with the i-region thicknesses labeled on the plot in μm.

from zero, E_{th} ($E^*_{th\ (e)} = 1.7$ eV and $E^*_{th\ (h)} = 1.6$ eV) while Li *et al.* [26] fitted the same theory to measured multiplication and noise data and found $E^*_{th\ (e)} = 2.1$ eV and $E^*_{th(h)} = 2.3$ eV which represents about 1.1 times E_{th}. In contrast, Spinelli *et al.* [27] calculated $E^*_{th\ (e)}$ and $E^*_{th\ (h)}$ in Si using a full-band Monte Carlo model and found their values to be 3 eV, about 2.5 times E_{th}, while realistic band-structure calculations also predict that most carriers in GaAs contribute significantly to ionization only once they have gain energies > 3 eV as shown by Jung *et al.* [28]. In Table I, the values of $E^*_{th\ (e)}$ and $E^*_{th\ (h)}$ which we obtain from the ionization PDF's in the same way as in [27] are also almost twice the minimum threshold energy, E_{th}, used in (1). One might then question how Li *et al.*managed to fit the measured results in GaAs using significantly lower values of E^*_{th}: We believe that this was because of their choice of ionization coefficients. They obtained α^* by assuming $\alpha_{MC} = \alpha$ and using (4). However, dead-space information is already contained in α which causes $\alpha_{MC} > \alpha$ so Li *et al.* would have to use a value of E^*_{th} that was below its real value to reproduce the correct overall multiplication. Li *et al.* also assumed ideal p$^+$-i-n$^+$s in fitting to the measured data whereas our calculations show that a relatively significant voltage can be dropped in the depletion region of thin structures. To validate that the data in Table I indeed quantify the multiplication correctly, M_e and M_h were calculated using the recursive technique in [14], [15] for the range of ideal p$^+$-i-n$^+$s in each composition and the results were compared with those from the MC simulations. The agreement was excellent when $w \geq 0.1$ μm in all compositions and so, for brevity, is illustrated only for GaAs in Fig. 8. Only small differences are evident at M_e and $M_h < 5$ for the thinnest 0.05 μm structure which are attributed to the assumption that the dead-space can be modeled by a step-function as described by (3). In reality, the ionization probability turns on more gradually over about 200 Å as seen in Fig. 6. Moreover, E^*_{th} is slightly

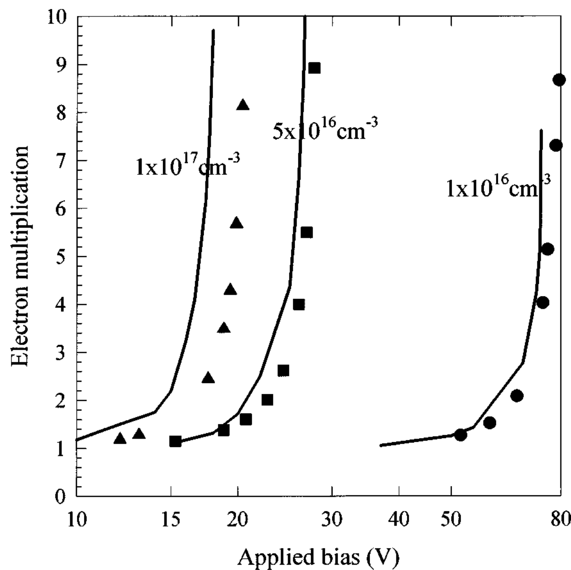

Fig. 9. Comparison of the $Al_{0.30}Ga_{0.70}As$ M_e curves calculated using the MC model (——) and a solution of the recursive equations (filled symbols) for three P^+N junctions where the n-doping is 1×10^{16} cm^{-3} (●), 5×10^{16} cm^{-3} (■), and 1×10^{17} cm^{-3} (▲). The n-doping values are also indicated on the plot in cm^{-3}.

larger ($\approx$ 10%) for primary carriers than the values given in Table I, since secondary carriers can have significant excess energy at their point of creation, but only one the value of E^*_{th} was used to give the data in Fig. 8. Both of these assumptions lead to the PDF description of (3) slightly overestimating the electric field corresponding to the onset of measurable multiplication in ultrathin devices.

Whereas the "microscopic" ionization coefficients can be used to calculate the multiplication in ideal p^+-i-n^+s, the applicability of these data to structures where the field varies rapidly is unclear. As mentioned previously, this is because the ionization probability of a carrier at any point depends on its history. The effects of field-tapers within a local model have already been identified by other authors including Beni and Capasso [29]. The assumption that α^* and β^* depend solely on the local field in the recursive technique would also be expected to become less accurate when field nonuniformity causes carriers to ionize at positions where they are not in equilibrium with the field. To estimate the potential error from neglecting the effect of carrier history, calculations of Me were carried out of for a range of abrupt one-sided $Al_{0.30}Ga_{0.70}As$ P^+N junctions doped at 1×10^{16} cm^{-3}, 5×10^{16} cm^{-3} and 1×10^{17} cm^{-3} using the MC model and compared with those predicted by the recursive technique. Since the recursive technique uses microscopic ionization coefficients, its implementation implicitly assumes that the probability that a carrier will ionize at a distance, z, where $z > d^*$, depends solely on the electric field at z. The results are compared in Fig. 9. As expected, when the field gradient is not appreciable the recursive technique gives reasonably accurate results but its applicability is more questionable as the field gradient increases. The curves from these calculations are displaced to the right of the MC curves by 1 to 2 V such that the relative error becomes restrictive when the doping is $> 5 \times 10^{16}$ cm^{-3}. This effect of a nonuniform field is difficult to circumvent with the recursive technique since it would require different PDF's to be tabulated in the computer program for each point along each new electric field geometry encountered. Since these would most probably have to be computed by a microscopic model beforehand, it might prove more computationally efficient to use a simple Monte Carlo model, such as those described in [16], [30], for such purposes. The errors from the recursive technique calculations in Fig. 9 represent a limitation to the accuracy of using α^* and β^* that depend only on the local field. However, further work is in progress to develop a practical description that allows the effects of field gradients to be accounted for when using field dependent ionization coefficients. Clearly, α^* and β^* will need to account for some memory of the carrier history when the field gradient is appreciable.

VI. Conclusions

A combination of accurately measured multiplication characteristics and an MC model have been used to extract the effect of alloy composition on the avalanche multiplication properties of $Al_xGa_{1-x}As$ $(x = 0 - 0.60)$. The main effect of increasing x is to displace the multiplication curves to higher electric fields for any given thickness. Both the relative change in the breakdown voltage and the voltage at the onset of measurable multiplication is similar for a given change in alloy fraction. The absolute dead-space distance increases with increasing alloy fraction. However, relatively less significant deviations from the local data are expected from materials with high alloy fractions and wide average band-gaps, since the dead-space distance represents a smaller fraction of the mean distance between ionization events.

Device-independent ionization coefficients are deduced for the first time, which are the inverse of the mean distance between ionization events in an infinite region of electric field. From these, the multiplication properties can be calculated for p^+-i-n^+s of an arbitrary thickness using a recursive technique. However, the assumption that these parameters depend solely on the local field causes errors when the electric field profile becomes highly nonuniform.

Acknowledgment

The first author is especially grateful for useful discussions with P. N. Robson from the University of Sheffield and D. C. Herbert at DERA.

References

[1] J. J. Chen, G.-B. Gao, J.-I. Chyi, and H. Morkoc, *Breakdown Behavior of GaAs/AlGaAs HBTs*, vol. 36, no. 10, pp. 2165–2172, Oct. 1989.
[2] M. J. Bailey, "Heterojunction IMPATT devices," *IEEE Trans. Electron Devices*, vol. 39, no. 6, pp. 1829–18348, Aug. 1992.
[3] C. Yeh and S. G. Liu, "Breakdown characteristics of $Al_xGa_{-1x}As$ diodes," *Appl. Phys. Lett.*, vol. 15, pp. 391–393, Dec. 1969.
[4] J. P. R. David *et al.*, "Measured ionization coefficients in $Ga_xAl_{1-z}As$," in *Proc. 1984 Symp. GaAs and Related Compounds, Inst. Phys. Conf. Ser.*, 1985, p. 247.
[5] V. M. Robbins, S. C. Smith, and G. E. Stillman, "Impact ionization in $Al_xGa_{1-x}As$ for x = 0–0.4," *Appl. Phys. Lett.*, vol. 52, pp. 296–298, Jan. 1988.

[6] A. Di Carlo and P. Lugli, "Dead-space effects under near breakdown conditions in AlGaAs/GaAs HBT's," *IEEE Electron Device Lett.*, vol. 14, pp. 103–105, Mar. 1993.
[7] S. A. Plimmer *et al.*, "Investigation of impact ionization in thin GaAs diodes," *IEEE Trans. Electron Devices*, vol. 43, pp. 1066–1072, July 1996.
[8] S. A. Plimmer *et al.*, "Impact ionization in thin $Al_xGa_{1-x}As$ ($x = 0.15$ and 0.30) P^+-I-N^+s," *J. Appl. Phys.*, vol. 82, pp. 1231–1235, Aug. 1997.
[9] K. A. Anselm *et al.*, "Performance of thin separate absorption, charge and multiplication avalanche photodiodes," *IEEE J. Quantum. Elec.*, vol. 34, pp. 482–490, Mar. 1998.
[10] D. S. Ong *et al.*, "A Monte-Carlo investigation of multiplication noise in thin p-i-n GaAs avalanche photodiodes," *IEEE Trans. Electron Devices*, vol. 45, pp. 1804–1810, Aug. 1998.
[11] K. A. Anselm *et al.*, "Characteristics of GaAs and AlGaAs homojunction avalanche photodiodes with thin multiplication regions," *Appl. Phys. Lett.*, vol. 71, pp. 3883–3885, Dec. 1997.
[12] G. E. Bulman, V. M. Robbins, and G. E. Stillman, "The determination of impact ionization coefficients in (100) gallium arsenide using avalanche noise and photocurrent multiplication measurements," *IEEE Trans. Electron Devices*, vol. ED-32, pp. 2454–2466, Nov. 1985.
[13] A. Spinelli and A. L. Lacaita, "Mean gain of avalanche photodiodes in a dead space model," *IEEE Trans. Electron Devices*, vol. 43, pp. 23–30, Jan. 1996.
[14] M. M. Hayat, B. E. A. Saleh, and M. C. Teich, "Effect of dead space on gain and noise of double-carrier-multiplication avalanche photodiodes," *IEEE Trans. Electron Devices*, vol. 39, pp. 546–552, Mar. 1992.
[15] M. M. Hayat, W. L. Sargeant, and B. E. A. Saleh, "Effect of dead space on gain and noise in Si and GaAs avalanche photodiodes," *IEEE J. Quant. Electron.*, vol. 28, pp. 1360–1365, May 1992.
[16] S. A. Plimmer, J. P. R. David, D. S. Ong, and K. F. Li, "The merits and limitations of local impact ionization theory, ," *IEEE Trans. Electron Devices*, vol. 45, pp. 1080–1088, May 2000.
[17] M. H. Woods, W. C.8 Johnson, and M. A. Lambert, "Use of a Schottky barrier to measure impact ionization coefficients in semiconductors," *Solid-State Electron.*, vol. 16, pp. 381–385, Jan. 1973.
[18] P. G. Scrobhaci and T.-W. Tang, "Modeling of the hot electron sub-population and its application to impact ionization in sub-micron silicon devices—Part I: Transport equations," *IEEE Trans. Electron Devices*, vol. 41, pp. 1197–1205, July 1994.
[19] M. Stobbe, R. Redmer, and W. Schattke, "Impact ionization rate in GaAs," *Phys. Rev. B*, vol. 49, pp. 4494–4497, Feb. 1994.
[20] J. Allam, "Universal dependence of breakdown voltage: Choosing materials for high power applications," *Jpn. J. Appl. Phys.*, vol. 36, pp. 15–29, Apr. 1997.
[21] S. Adachi, "GaAs, AlAs and $Al_xGa_{1-x}As$ material parameters for use in research and device applications," *J. Appl. Phys.*, vol. 58, pp. 1–29, 1985.
[22] S. M. Sze and G. Gibbons, "Avalanche breakdown voltages of abrupt and linearly graded pn junctions in Ge, Si, GaAs and GaP," *Appl. Phys. Lett.*, vol. 8, pp. 111–113, 1966.
[23] D. C. Herbert, "Breakdown voltage in ultra-thin pin diodes," *Semicond. Sci. Tech.*, vol. 8, pp. 1993–1998, 1993.
[24] R. Ghin *et al.*, "Avalanche multiplication in $Ga_{0.52}In_{0.48}P$ diodes," *IEEE Trans. Electron Devices*, vol. 45, pp. 2096–2101, Apr. 1998.
[25] D. S. Ong, K. F. Li, G. J. Rees, J. P. R. David, and P. N. Robson, "A simple model to determine multiplication and noise in avalanche photodiodes," *J. Appl. Phys.*, vol. 83, pp. 3426–3428, Aug. 1998.
[26] K. F. Li *et al.*, "Avalanche multiplication noise characteristics in thin GaAs p-i–n diodes," *IEEE Trans. Electron Devices*, vol. 45, pp. 2102–2107, Oct. 1998.
[27] A. Spinelli, A. Pacelli, and A. L. Lacaita, "Dead-space approximation for impact ionization in silicon," *Appl. Phys. Lett.*, vol. 69, pp. 3707–3709, Dec. 1996.
[28] H. K. Jung, K. Taniguchi, and C. Hamaguchi, "Impact ionization model for full band Monte-Carlo simulation in GaAs," *J. Appl. Phys.*, vol. 79, pp. 2473–2480, Mar. 1996.
[29] G. Beni and F. Capasso, "Effect of carrier drift velocities on measured ionization coefficients in avalanching semiconductors," *Phys. Rev. B*, vol. 19, pp. 2197–2203, 1979.
[30] S. A. Plimmer, J. P. R. David, D. S. Ong, and K. F. Li, "A simple model for avalanche multiplication inclusing deadspace effects," *IEEE Trans. Electron Devices*, vol. 46, pp. 769–775, Apr. 1999.

Stephen A. Plimmer was born in Stoke-on-Trent, U.K., in 1972. He received the B.Sc. (Hons.) degree in physics and the Ph.D. degree in electronic engineering from the University of Sheffield, U.K., in 1993 and 1997, respectively. His doctoral work focused on experimental and theoretical study of impact ionization in $Al_xGa_{1-x}As$ ($x = 0 - 0.9$).

He now works as an Research Associate at the University of Sheffield, where his main topic is single photon avalanche detectors (SPAD's).

John P. R. David received the B.Eng. and Ph.D. degrees from the Department of Electronic and Electrical Engineering, University of Sheffield, Sheffield, U.K., in 1979 and 1983, respectively.

In 1983, he joined the Department of Electronic and Electrical Engineering, University of Sheffield, where he worked as a Research Assistant investigating impact ionization. In 1985, he became responsible for characterization within the SERC (now EPSRC) Central Facility for III–V Semiconductors at the same university. His current research interests are piezoelectric III–V semiconductors and impact ionization in bulk and multi-layer structures.

Robert Grey received the B.Sc. degree in physics and the Ph.D. degree from the University of Newcastle, U.K., in 1973 and 1977, respectively.

From 1977 to 1988, he was with VG Instruments initially as a Test and Development Scientist, then as a Molecular Beam Epitaxy (MBE) Engineering Manager, and finally taking the role of customer services manager. He moved to the SERC Central Facility for III-V semiconductors as an MBE semiconductor crystal grower in 1988, where he provides semiconductor structures for U.K. and international physics and electronics device groups.

Graham J. Rees received degrees in physics and theoretical physics from Oxford University, Oxford, U.K., and Bristol University, Bristol, U.K.

He has since been with Rome Universita della Scienze, Imperial College London, Plessey (now GEC) Caswell, Lund University, Sweden, and Oxford University. He is currently a Professor at the University of Sheffield, Sheffield, U.K. His interests are in the physics of semiconductors and devices.